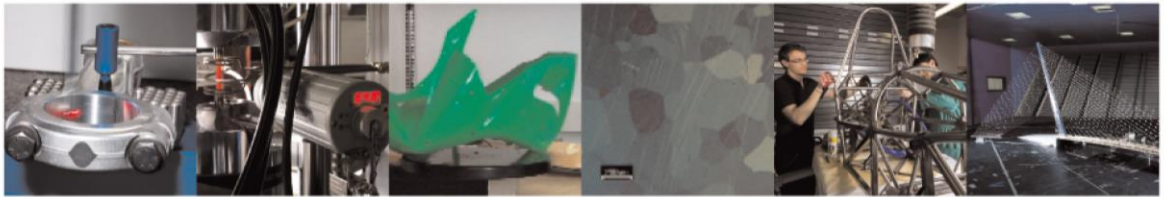




POLITECNICO
MILANO 1863

DIPARTIMENTO DI MECCANICA



On The Combined Use Of Digital Image Correlation And Micro Computed Tomography To Measure Fibre Orientation In Short Fibre Reinforced Polymers

A. Bernasconi, M. Carboni, R. Ribani

This is a post-peer-review, pre-copyedit version of an article published in Composites Science and Technology. The final authenticated version is available online at:

<https://doi.org/10.1016/j.compscitech.2020.108182>

This content is provided under [CC BY-NC-ND 4.0](https://creativecommons.org/licenses/by-nc-nd/4.0/) license



On the combined use of Digital Image Correlation and Micro Computed Tomography to measure fibre orientation in short fibre reinforced polymers

A. Bernasconi^{1,*}, M. Carboni¹, R. Ribani¹

¹Politecnico di Milano, Dipartimento di Meccanica, Via La Masa 1, 20156 Milano, Italy

*corresponding author: andrea.bernasconi@polimi.it

Abstract

Measurement of fibre orientation in short fibre reinforced polymer is crucial for the description of their microstructure and subsequent multiscale modelling. Micro Computed Tomography is becoming the standard method for the reconstruction of the inner microstructure of short fibre reinforced polymers and different methods exist for the analysis of orientations. Applications of Digital Image Correlation to X-rays Micro Computed Tomography data sets to measure fibre orientation in continuous fibre reinforced polymers exist. In this work, the possibility of extending the application of the Digital Image Correlation technique to measure fibre orientation in short fibre reinforced polymers is investigated and a new procedure is proposed. The method is applied to two different data sets obtained by scanning the same sample using both a synchrotron micro CT equipment and an industrial scanner. Results are compared with other existing methods and discussed to identify possible future improvements.

Keywords: short fibres, polymers, injection moulding, x-rays micro computed tomography, fibre orientation, digital image correlation

1 Introduction

Short fibre reinforced polymers (SFRP) are more often chosen for the design of load bearing, lightweight parts in many industrial fields. The main advantages consist of feasibility of

complex shapes with short manufacturing times coupled with high specific mechanical properties [1]. Knowledge of the mesostructure is required to predict quantitatively composites' mechanical properties [2]. Particularly, the fibre orientation distribution (FOD) is crucial as the strengthening effect of fibres is maximum when the fibres are aligned with the stresses acting in the component, resulting in an anisotropic material behaviour. Models for predicting SFRPs' properties based on their microstructure have been developed [3] and they require accurate knowledge of fibre orientation.

The manufacturing process, usually injection moulding, controls the FOD and the properties of the final component [4]. Fibres are oriented by the dynamics of the molten reinforced polymer as it fills the mould. In regions of shear flow, close to the mould's walls, fibres tend to align with the flow direction, while in regions of extensional flow, typically the core layer, fibres tend to align perpendicular to the flow [5, 6]. The effects of this layered structure on the mechanical properties are reported in [7].

1.1 Experimental methods for measuring fibre orientation

In injection moulded real parts, the fibre orientation has a strong influence on the mechanical performances. For example, as reported in [8], the specimens studied in this work, being characterized by the above mentioned layered structure, are 21% less stiff and 15% less strong than standard ISO 527 type1A specimens of the same material, that have a more uniform fibre orientation along all the side walls. Real parts have complex geometries, with thin walls intersecting along edges that are rounded with relatively small fillet radii. In these regions stress concentrations usually appear and the melt polymer flow is disturbed and so is FOD. To predict the FOD in real parts, the injection moulding process can be simulated. Furthermore, in Finite Element Analyses (FEA) it is possible to assign local properties to the elements based on predicted FOD [7]. In this context, the orientation tensor is usually chosen

to describe the fibre orientation [2, 9]. By combining process simulation and FEA, i.e. by the so called Through Process Modelling, it is possible to optimize the orientation of the fibres with respect to the stresses acting in the real part, by proper selection of the number, position and type of injection gates. However, the values of the orientation tensor obtained by process simulation must be checked against measurements on real parts to assess their validity, particularly at the above-mentioned locations and possibly over large volumes. For this purpose, several different methods exist.

1.1.1 Optical methods

Optical methods are mainly based on observation of polished surfaces of physical sections [10], resulting in a fully destructive technique. The orientation of each fibre is estimated by measuring the orientation and the length of the major and minor axes of the elliptical fibre footprints left on the sectioning plane. Contact microradiography [11] and microscope imaging [12] have been used. Specific automated systems exist to scan large areas [13]. Contrast enhancing techniques, like polishing and etching with oxygen ions [14], are required to obtain accurate measurements. Some sources of error have been identified [15, 16]. Measurement error increases as the fibre tends to be perpendicular to the cutting plane [17] and the sensitivity of the measured out-of-plane angle to small errors in the determination of ellipse axes increases non-linearly when the angle tends to zero [15,16]. Moreover, there is a 180° uncertainty for the in-plane angle and therefore not all orientation tensor components can be evaluated [17]. To overcome this ambiguity, some authors analysed couples of parallel or perpendicular sections [18], while others tried to obtain 3D reconstructions through successive sectioning [19] or polishing [20]. To avoid issues related to inaccurate successive section registration, confocal laser scanning microscopy [17, 21, 22] or shadow scanning electron microscopy [23] was used. The optical methods allow for scanning relatively large

areas, but are a fully destructive method and, unless the above-mentioned special techniques are applied, do not allow to measure all the fibre orientation tensor components.

1.1. 2 Methods based on Micro Computed Tomography

Micro Computed Tomography (micro-CT) can provide a 3D reconstruction of the external and internal material structure. The FOD analysis methods based on micro-CT can be subdivided into three groups.

The first one tries to distinguish each single fibre to calculate its orientation [24-27]. These methods based on single fibre segmentation allow for the calculation of the complete FOD; however, they require a very high spatial resolution. Robust and accurate results were achieved with a resolution of 1 μm on a scan domain of $(2000 \mu\text{m})^3$ corresponding to a full height scan of a 2 mm thick injection moulded plate [27]. At present, the high resolution required compared to the dimension of the available sensors considerably limits the dimensions of the scan volume.

The second group analyses 2D slices extracted from the volume. In [28], fibre orientation was evaluated based on the difference of intensity along two perpendicular directions at boundaries between fibres and matrix. However, out of plane angles cannot be measured. To do so, a manual method, based on the analysis of several 2D slices, was proposed in [29]. In the present work, the Directionality plug-in of Fiji/ImageJ software package (simply identified as “Directionality” in the following) was used. It belongs to this class and it infers the preferred orientation of structures in 2D images, calculating a histogram indicating the amount of structures in a given direction. The image is chopped into square pieces and their Fourier power spectra are computed, which are analysed in polar coordinates using appropriate spatial filters to obtain the orientation histogram. These algorithms do not require

high resolution and therefore allow for larger scan areas. However, they do not allow to measure 3D distributions and are mainly suitable for planar distributions.

The third group analyses the whole 3D reconstructed volume, entirely or subdivided in small domains, by methods that can be defined as indirect, because they do not rely on the segmentation of each single fibre. These methods can determine fibre orientation also when spatial resolution is low, allowing to increase the speed of the analysis or the size of the volumes. The Mean Intercept Length (MIL) concept was applied in [30], allowing to evaluate the MIL fabric tensor. This method was compared with optical methods in [31]. Anisotropic Gaussian filtering [32], inertia tensor [33] or structure tensor [34-36] can also be used to determine the local orientation of fibres. The Hessian matrix, calculated as the dyadic product of the second partial derivatives of the grey values, can be used for estimating local fibre directions [26]. The eigenvector corresponding to the smallest Hessian matrix eigenvalue can be used as an estimator of the local fibre direction. Anisotropic Gaussian filter, structure tensor, Hessian matrix methods [37] and main axis of inertia method were compared [38]. The Fibre composite material analysis module of the software VGStudio MAX (by Volume Graphics) allows to evaluate global and local fibre orientation distributions exploiting these types of methods, for example the Hessian matrix. It has been used in this work to obtain 3D measurements, which do not assume that the FOD is planar as Directionality does.

All these methods are micro-destructive. The integrity of the volume is preserved, but a small volume, generally a cube of a few millimetres edge length, needs to be extracted from the part. Indirect methods have less stringent requirements for the spatial resolution of the scan. For example, results consistent to those obtained with a single fibre segmentation method were obtained using the structure tensor with resolutions varying from 1.4 to 16 μm on a scan volume of $2611*2436*655 \mu\text{m}^3$ [36]. The maximum dimensions of the volume that can be

analysed are at present limited by the imaging, memory and computational resources of available computers.

A method allowing for scanning even larger volumes still has to be proposed and, in this paper, we explore the potential of a method based on Digital Image Correlation (DIC), which in principle could allow for measuring FOD over larger volumes than with the aforementioned methods and can make use of already available DIC software packages.

DIC was used to measure fibre orientation in micro-CT reconstructed volumes of composite materials in [39], to analyse a quasi-isotropic CFRP laminate stacking configuration of $[45/0/-45/90]_{4S}$ and a plain woven CFRP laminate, both characterized by the presence of long fibres having the same local orientation. The method was also applied to measure fibre waviness in unidirectional CFRPs [40], whereas in [41] fibres' cross sections were tracked by a semi-automated method.

Digital Image Correlation is a full-field optical metrology based on digital image processing and numerical computing [42]. It is usually employed to measure surface displacements of an object under mechanical or thermal loads. It requires that the surface of the object is covered by an irregular pattern of dark dots on a white background (speckle). Images of the surface are taken during loading and the image is divided into subsets. By analysing digital images taken in a non-perturbed condition (reference image) and in perturbed condition (correlated images), the positions of image subsets can be tracked across several images and finally a displacement field can be reconstructed.

To measure fibre orientation in composite materials by DIC applied to micro-CT reconstructed volumes, the variations of radiation intensity, related to the different attenuation of fibre and matrix, are exploited as a natural speckle. In principle, two adjacent and parallel slices of a volume reconstructed after an x-rays micro-CT scan (see Figure 1)

would suffice to evaluate fibre orientations, without limitations on the size of the slice (the only limitation being the maximum size of the material volume analysable by the available micro-CT equipment). This is the case of the material reinforced by continuous fibres studied in [39], where all the fibres can be reasonably assumed to have the same orientation.

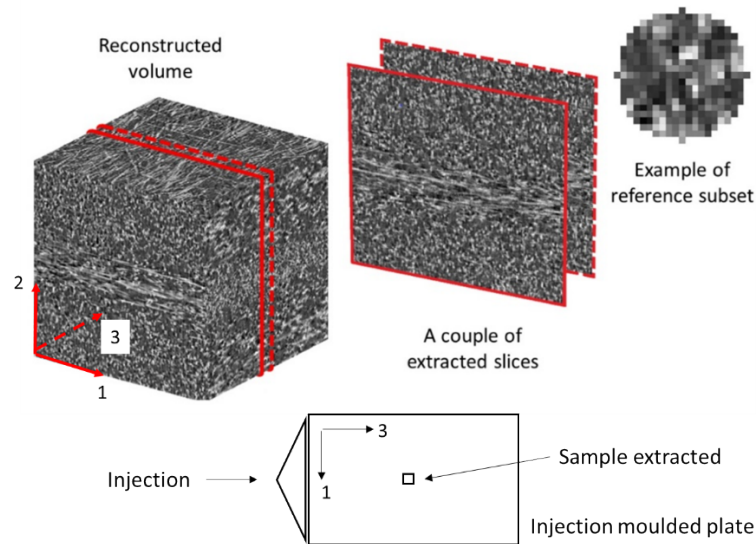


Figure 1 – Reconstructed volume, two adjacent slices and a DIC subset

In SFRPs, the method is not applicable in a straightforward manner, because the fibre distribution pattern is more complex than in unidirectional composites. The fibres are shorter, discontinuous, with a non-uniform fibre distribution inside the reference volume and variable across the thickness of the sample. Therefore, in this work, we modified this method to make it applicable to injection moulded short fibre reinforced polymer and to check its ability to measure non-uniform FODs, geometrically more complex than those analysed in [39]. The application to SFRP required the development of a novel procedural approach that was checked against the results obtained on the same sample using Directionality and VGStudioMax, that are based on the fibre orientation methods described in the previous sections. The new method was applied to a sample of injection moulded short glass fibre reinforced polyamide. However, there are no restriction to the applicability to other polymer

matrices, either thermosetting or thermoplastics, because all polymers have similar X-ray absorption coefficients, provided that CT scans allow for sufficient contrast between the matrix and the fibres. Therefore, limitations are expected for polymer fibres and carbon fibres, whose X-ray absorption coefficient is closer to that of polymer matrices with respect to glass. In the case of carbon fibres, limitations can be overcome by contrast enhancing techniques like phase contrast [43, 44].

2 The use of DIC to measure FOD in composites

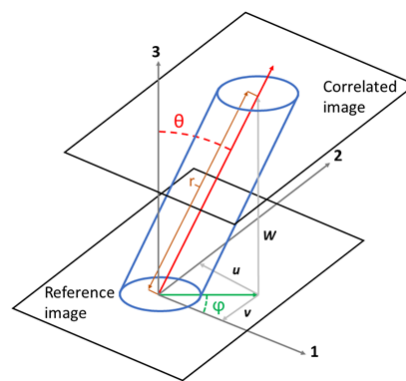


Figure 2 – Example of fibre orientation calculation by DIC and reference system

The principle that can be applied can be illustrated with reference to a simple case where it is supposed that one subset contains the trace left by one single fibre (Figure 2). Being u and v the measured displacement components in the slicing planes of the trace of a single fibre and w the distance between the two planes, the fibre orientation is defined by the angles θ and φ :

$$\theta = \text{atan} \left(\frac{\sqrt{u^2 + v^2}}{w} \right) \quad (1)$$

$$\varphi = \text{atan} \frac{v}{u} \quad (2)$$

As already mentioned before, to apply DIC, the radiation intensity distribution resulting from fibres and matrix is used as a natural speckle. In most cases, tracking each single fibre is not possible, because a single subset must contain enough information to be sufficiently different

from the other subsets so that it can be traced without ambiguity. If all the fibres in a subset have the same orientation, the measurement of their orientation by DIC is not affected by the subset size. If, as it is often the case, they have different orientations, the size of the subset becomes crucial, because large subsets are likely to average the orientations over the subset. Therefore, in the case of large FOD gradients over the subset, the accuracy of FOD measurements may decrease with increasing subset size.

2.1 Limitations of a direct DIC approach

In the case of long fibres having the same local orientation, two adjacent slices, of any size, would suffice to evaluate fibre orientations, thus making it possible to scan large areas.

However, in the case of short fibres, a more complex fibre distribution is found. This leads to sources of error that prevent from applying the method to a set of just two adjacent slices (Figure 3). For example, when fibres are almost parallel to the plane of the slices, some of them are likely not to be found in the reference and the correlated ones at the same time.

Furthermore, the higher the angle between the fibres and the normal to the reference slice, the higher the chance for the fibres to be lost in the correlated slide with respect to the reference one. This could lead to the inability of the DIC to measure accurately large fibre angles (based on the authors' experience, if it is greater than 30°). Moreover, it is possible that the trace of another fibre is found in the correlated slice and, therefore, the angle is measured as a smaller one.

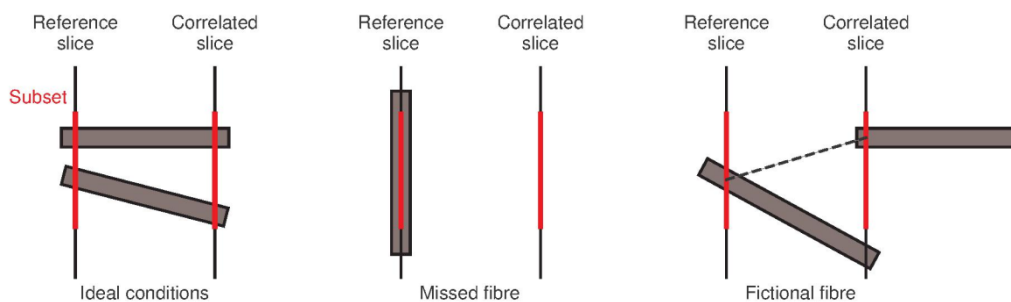


Figure 3 – Schematic example of fibre tracing errors

3 The proposed procedure

To overcome these issues, a new procedure is proposed. The present procedure is valid for samples extracted from locations where the fibre orientation distribution tends to be planar, e.g. from plates, from thin side walls or from reinforcing ribs of hollow structures. First, a segment is chosen along which the FOD is computed. This base segment should be perpendicular to the midplane of the part. Then, several cross sections of the micro-CT reconstructed volume belonging to the sheaf of planes whose axis is the base segment (Figure 4 -a) are chosen, making a full revolution with a certain angular step. Each section (slice) works as reference image for a DIC test performed between it and another section (slice) taken parallel to it at a given small distance w . ImageJ/Fiji plugin Volume Viewer was used to reconstruct the analysed specimen and to extract slices at various orientation. The angle step was set to 5° , as a trade-off between required computational time and angle resolution.

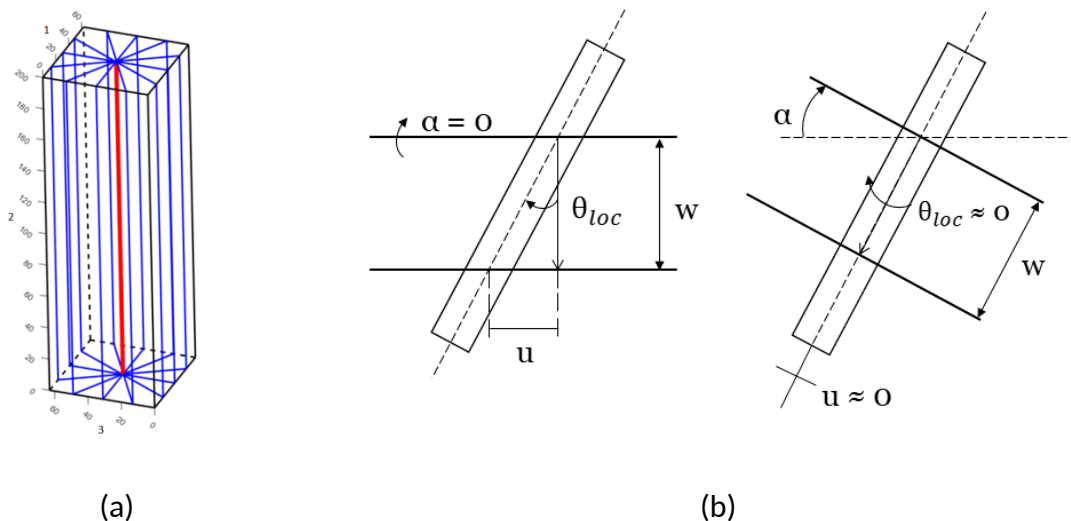


Figure 4 – (a) base segment (in red) and sheaf of reference planes (in blue); (b) 2D scheme of search of the minimum local θ angle

For each orientation α of the reference cross section, displacements were evaluated by DIC using the nCorr open source 2D DIC Matlab program (www.ncorr.com) and values of the angle θ were evaluated in the local reference frame using Eq. (1) and defined as local angle θ

θ_{loc} values. Once DIC measurements are performed for all the orientations of the reference section, only the measured displacements resulting in the minimum (possibly zero) local angle θ_{loc} are assigned to each measurement point along the base segment (Figure 4 -b). This ensures that the θ_{loc} angle is measured with the smallest error, as it was shown that large angles are likely not to be measured accurately by DIC. The orientation of the section that minimizes θ_{loc} is recorded. Then, the displacements measured with respect to this orientation are transformed into the global reference frame and finally the global θ and φ angles are computed. This process is repeated for each point along the base segment. If the base segment cannot be chosen such that the fibre orientation distribution is as planar as possible in each plane perpendicular to the segment, the proposed procedure cannot be applied. This issue needs to be addressed in the future, e.g. by using a 3D grid of several segments or by extracting, with appropriate angular steps in local spherical coordinates, all planes passing through each measurement point.

3.1 Filtering of the correlation coefficient

The procedure presented above cannot distinguish low θ_{loc} angles, corresponding to a true minimum of the local orientation, from θ_{loc} angles resulting from inaccurate measurements, usually generated by very large real orientation angles. The correlation coefficient is used to distinguish these cases. The greater the similarity between the reference subset and the correlated one, the lower the corresponding correlation coefficient evaluated by DIC. The systematic error arising from large θ angles is caused by a miss-tracing of the subset; in this case, a larger value of the correlation coefficient is expected. Therefore, a threshold value for the correlation coefficient is set and any measurement characterized by a correlation coefficient larger than the threshold is discarded.

In this work, it was found that an appropriate threshold can be expressed as a fraction of the mean correlation coefficient resulting from the DIC tests at all slices' orientation angles. Several fraction values of the mean correlation coefficient were tested, and the threshold was identified as the value that ensured the best agreement between DIC, Directionality and VGStudio MAX results with respect to the main orientation angle. However, this procedure requires a comparison with other methods and the optimum value might depend on the parameters of the micro-CT scan. An independent filter definition based just on the information deriving from DIC results should be developed in the future to improve performances of this procedure even without a comparison method.

3.2 Subset size and averaging results over adjacent subsets

The choice of the subset size requires that it is small enough to capture gradients, but large enough to allow for good correlation. In the following examples the size was determined by a convergence analysis, as the minimum size that allowed for stable and smooth results. The final value has been kept equal across all the tests presented here, with just small variations since the radius must match an integer number of pixels to perform DIC.

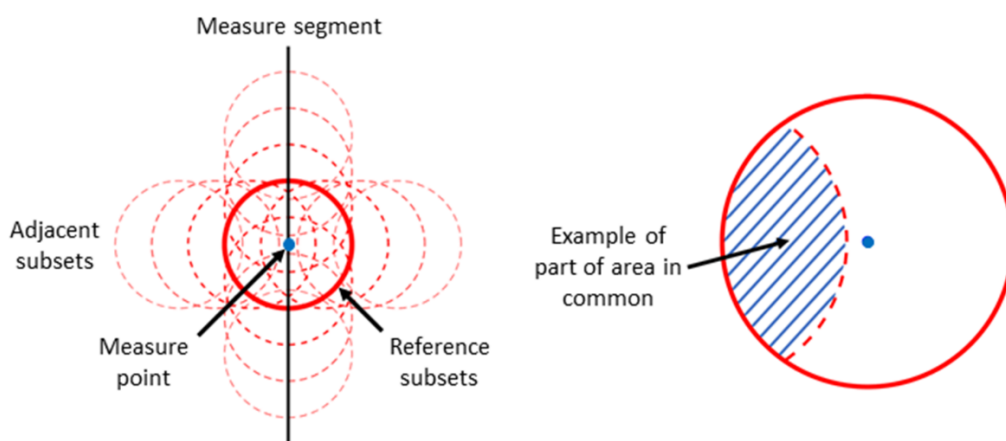


Figure 5 – DIC subset superposition

Fibre orientation tensor components are defined as average values of functions of the orientation angles of fibres inside a representative volume element, and they are capable of describing fibre orientation distributions ranging from fully aligned fibres to random distributions. Instead, DIC assigns the same orientation to all the fibres inside each subset, resulting in a locally perfectly unidirectional FOD. In an attempt to capture the non-uniformity of fibre orientation around each point of measurement, the tensor has been calculated as a weighted average between the local tensor evaluated in the subset centred on the point of measurement and the ones calculated in the adjacent points along the base segment and perpendicularly to it. The weights are equal to the portion of the common area between the adjacent subsets and the reference one in the slice image (Figure 5).

3.3 Methods used for comparison of results

Directionality was first used to compare results obtained with the proposed procedure. It was applied to planar sections of the reconstructed volumes. The orientation histogram evaluated by Directionality over square subsets of the images was assumed as a FOD to calculate the fibre orientation tensor. As Directionality calculates the FOD based on a 2D image, the hypothesis of planar fibre distribution must be made (the φ angle is set to 0) and sections extracted perpendicular to the measure segment are analysed. Thus, DIC and Directionality planes were perpendicular to each other.

Fibre orientation tensor components could be evaluated by Directionality at each point along the base segment. However, to compare results obtained by DIC on volumes of comparable size, the Directionality subset analysed had the side equal to the DIC subset diameter and then the values of the orientation tensors were averaged over a stack of few adjacent planes in a range equal to the DIC subset diameter.

To obtain full 3D measurements, the fibre composite material analysis module of VGStudio MAX software by Volume Graphics was also used. First, a grey scale threshold was applied to perform a fibre surface determination. A region of interest was defined around the measurement segment and it was divided in several rectangular parallelepiped subsets which do not overlap each other. For each subset, the orientation tensor was evaluated using the analysis module. To ensure the maximum agreement between the volumes analysed through DIC and VGStudio MAX, the dimensions of the rectangular parallelepiped perpendicular to the measure segment were set equal to the DIC subset diameter, whereas the dimensions along the measurement segment were set to half the DIC subset diameter, rounded up to the first integer number. This was chosen as a trade-off between noise (smaller subset) and resolution (larger subset).

4 Application of the proposed procedure to a SFRP sample

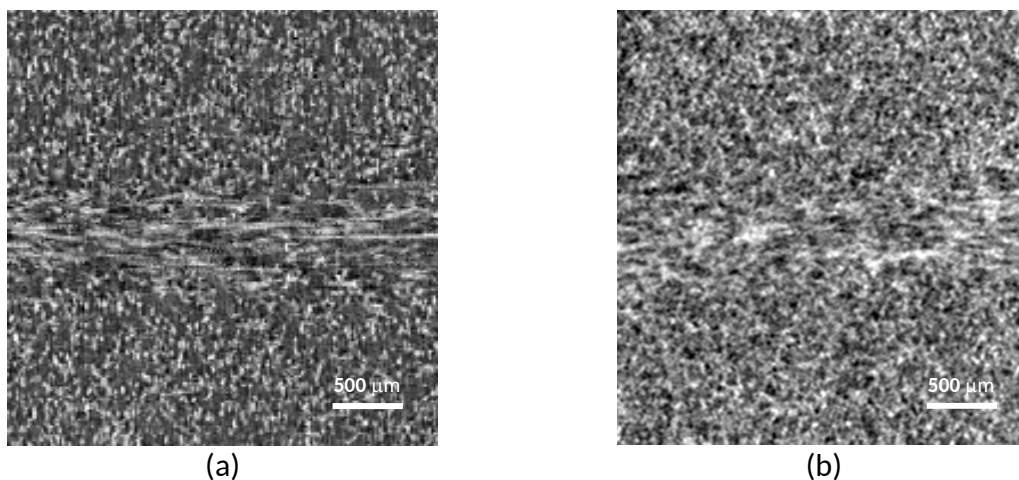


Figure 6 – (a) a slice from the sample reconstructed through synchrotron radiation; (b) a slice from the sample reconstructed with a commercial micro-CT

The proposed method was applied to a sample extracted from an injection moulded plate of 120 mm x 180 mm injected through a funnel gate located along the shorter edge. The sample is made of PA6 (polyamide 6) reinforced by a 30% weight fraction of short E glass fibres, having a nominal diameter of 11 μm ; as reported in [30], fibre diameter values follow a

Gaussian statistical distribution with a mean value of 10.5 μm and standard deviation of 2 μm . Fibre length values follow a Weibull distribution with a weighted average fibre length of 275 μm [45]. The sample is the prism of 3.1 x 3.6 x 12 mm analysed in [30], where more details can be found. The same sample was scanned using two different micro-CT equipment. The first time, the volume was the one that had been reconstructed by micro-CT at the SYRMEP beamline of Elettra (Trieste, Italy) using synchrotron radiation [30]. The voxel size is 9 μm . Figure 6(a) showcases a slice of the reconstructed volume, with the typical shell-core-shell structure. Phase contrast was exploited in the reconstruction of this data set.

Then, the same sample was CT-scanned using a GE Baker Hughes Phoenix v|tome|x m commercial tomographic equipment, as well, to demonstrate its applicability when using a less expensive instrument. The sample was CT-scanned with a voltage of 70 kV and a current of 100 μA , resulting in a power of 7 W and a focal spot size of 7 μm . The distances chosen are tube to detector 807.51 mm and tube to part 39.82 mm, resulting in a zoom factor of x20.28 (4.9 μm of voxel size). The proposed procedure for fibre orientation analysis was applied with a subset radius of 95 μm for DIC. As shown in Figure 6(b), the slice extracted from the volume reconstructed through the commercial micro-CT appear noisier, with lower contrast, although a normalization was performed to enhance contrast. In fact, the contrast of the images obtained by synchrotron X-ray tomography is improved by phase contrast imaging, resulting into a better visualization of the fibres even if the voxel size is larger than that of the commercial equipment.

Orientation tensors are used to compare the measurement performed by the three considered methods: DIC, Directionality and VGStudio MAX. Directionality was used also in the calibration phase (threshold for the correlation coefficient), while VGStudio MAX was used as a further validation. First, tensor elements a_{11} , a_{22} , a_{33} and a_{13} were compared. When fibres

are highly aligned with the direction i , the tensor element a_{ii} tends to 1. a_{13} is proportional to the angle in the plane 1-3 between the principal fibre orientation reference system and the considered global reference systems. In the cases analysed herein, axis 3 is aligned to the main axis of the plate from which the sample is extracted (flow direction), axis 2 is oriented through the thickness of the plate and axis 1 is perpendicular to the main axis of the plate. Useful information can be extrapolated also from the first eigenvector of the fibre orientation tensor. It represents the main direction of orientation and its θ and φ angles can be utilized for comparison.

4.1 Sample scanned at Elettra Synchrotron

First, the inability of DIC to measure large θ angles from a single pair of consecutive slices is demonstrated. Two slices were extracted perpendicular to the flow direction: the maximum local θ angle measured in the core was about 45° , well below the expected value in the core region of about 90° . Along the line highlighted with red dash in Figure 7a, the local θ angle calculated by DIC does not reach 30° (Figure 7b), while Directionality and VGStudio MAX captured well the expected rotation by 90° in the core, consistent with the qualitative orientation shown in Figure 6.

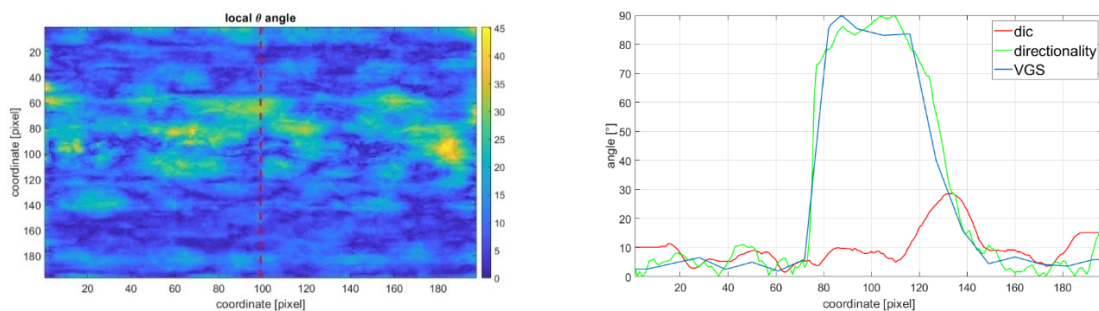


Figure 7 –map of the local θ angle (a) and values angle along the measure segment (b)

Then, the proposed algorithm was applied. A threshold of 0.16 was found, that ensured the best agreement with Directionality and VGStudio Max in terms of the first principal direction

of the orientation tensor, as described in section 3.1. It corresponds to 68% of the average value of the correlation coefficient over all angles. The values of the orientation tensor components obtained by this method are reported in Figure 8.

Values of a_{11} , are higher for Directionality than for VGStudio MAX and a_{22} is equal to zero for Directionality, because out-of-planes angles cannot be measured by this method. Values of a_{11} and a_{33} show a qualitative agreement between DIC and the other methods. The layered structure of the sample is captured, but DIC yielded tensor values which are characterized by higher extreme values than the other two methods. The method seems to overestimate the orientation uniformity inside the analysed volume, even if the averaging method described in section 3.2 was applied. a_{22} DIC values are very low and they are closer to the one estimated by Directionality. Finally, higher a_{13} values have been obtained through DIC, indicating that the method measures a greater mismatch between the global reference system and the principal one with respect to Directionality.

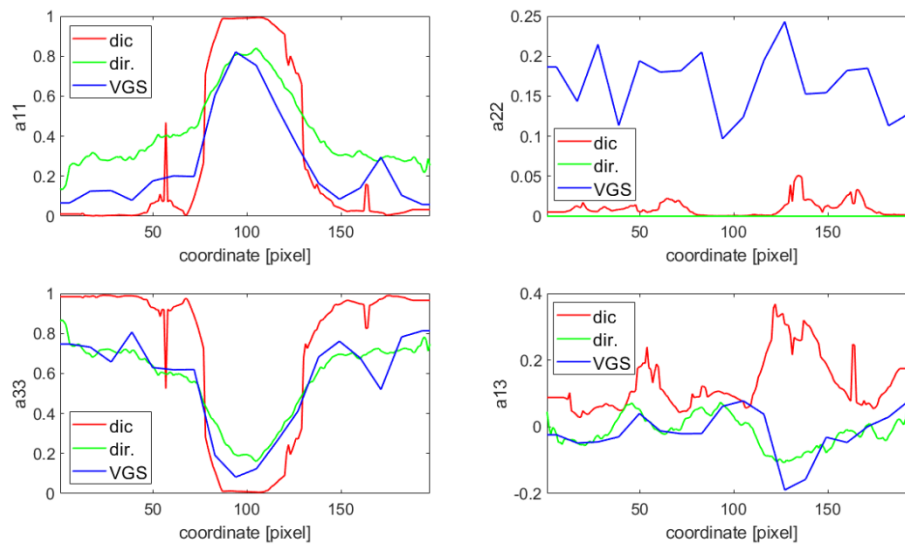


Figure 8 – tensor elements on measure segment obtained from synchrotron scan

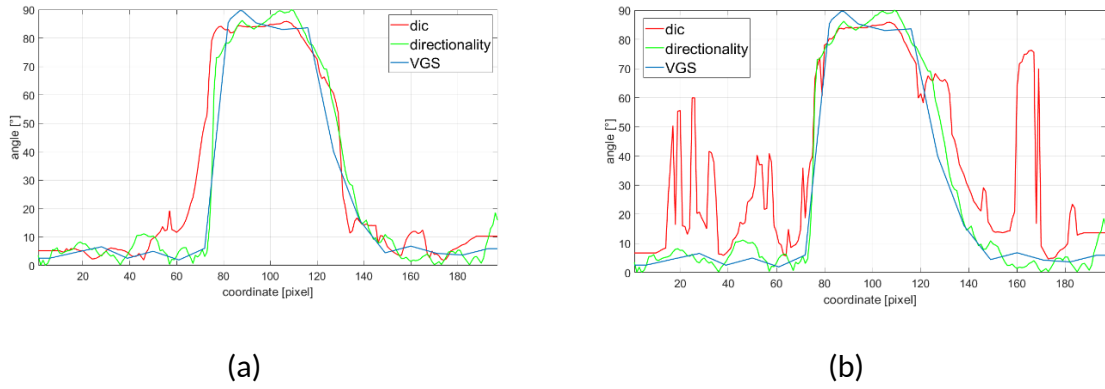


Figure 9 – main θ angle on measure segment obtained from synchrotron scan with filter (a) and without filter (b)

As for the value of the first principal direction, a good agreement between the three methods was found (Figure 9-a). It appears that DIC tends to slightly overestimate the thickness of the transition zone between the shell and the core layers. The main effect of the filter applied on the correlation coefficient is to improve the results, removing errors especially in the shell regions, as it can be noted in Figure 9-b.

4.2 Sample scanned using an industrial micro CT scanner

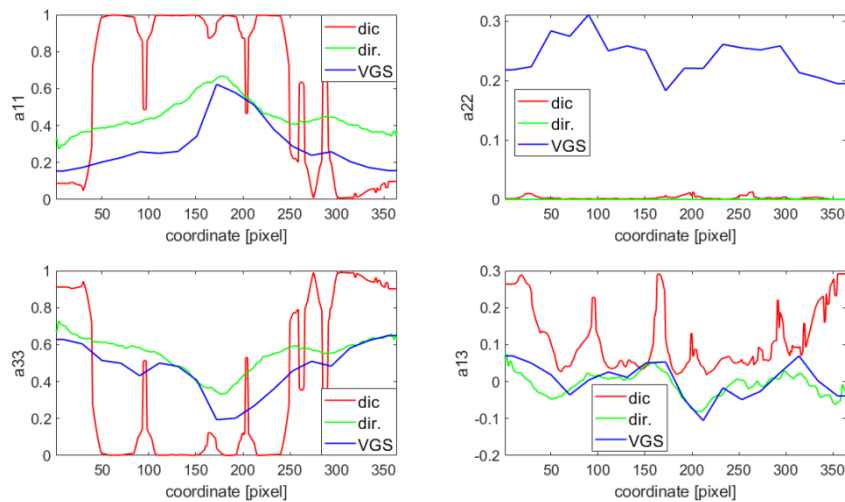


Figure 10 – tensor elements on measure segment obtained from commercial micro-CT scan

The fraction value of the mean correlation coefficient which ensured the best agreement between results was equal to 0.675, the same as for the previous test, which results in a filter threshold of 0.04. In Figure 10, the results in terms of orientation tensor elements for this test are reported. Also in this case, the two control methods show a good agreement in measuring orientation tensor elements, even though slightly higher discrepancies are present. For what concerns DIC measurements, contrary to the previous test, a_{11} and a_{33} show a poorer agreement with the results obtained with the other control methods. Nevertheless, the layered structure of the sample can be guessed also from DIC, even if the uniformity of the orientations is strongly overestimated. By scanning the sample with a commercial micro-CT, worst results were expected due to the lower contrast resulting in the final reconstructed volume, a fundamental parameter to obtain reliable results with DIC algorithm, in spite of a smaller voxel size.

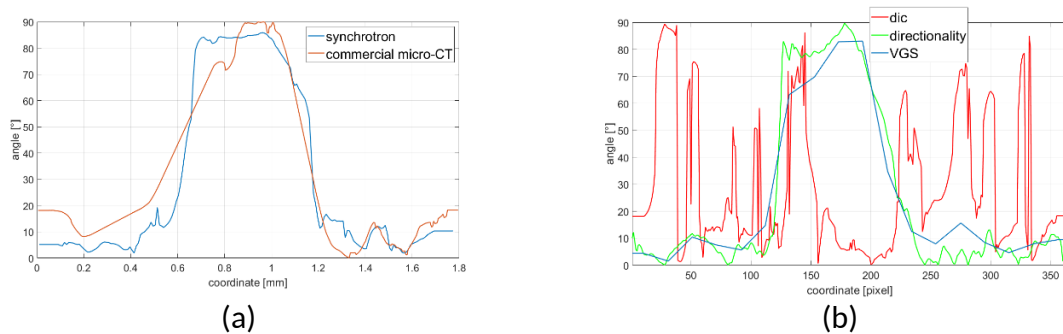


Figure 11 – main θ angle on measure segment obtained from commercial μ -CT scan with filter compared with synchrotron (a) and without filter (b)

A better agreement was found between the values of the main orientation direction using the commercial scanner and the Synchrotron beamline, as shown in Figure 11-a. The position and the thickness of the core region is very similar. Also in this case, the filter on correlation coefficient is necessary to obtain meaningful results. As it can be seen from Figure 11-b, the results obtained if the filter is not applied are quite random. The capability of identifying the shell-core-shell structure along the base segment also under these experimental condition

shows the potential applicability of the proposed method even using more affordable laboratory equipment, provided that the evaluation of the values of the fibre orientation tensor components is improved. To achieve this, future improvement should probably be focused on the procedure for averaging the orientations angles over the adjacent ROIs.

5 Concluding remarks

The possibility of using DIC to measure FOD in samples of SFRPs reconstructed by micro-CT was thoroughly investigated. The method is applicable to any combination of polymer matrix and short fibre systems, provided that CT scans allow for sufficient contrast between the matrix and the fibres. The interest in the DIC based method stemmed from the possibility of analysing large volumes in the case of continuous fibres. Difficulties arise when trying to exploit as a natural speckle the footprints left by short fibres onto two adjacent slices of a reconstructed 3D image of the internal structure of a material sample. A possible procedure that sought to overcome these difficulties was proposed. Two data sets of the same sample were employed, obtained using Synchrotron radiation and a standard micro-CT scanner. Synchrotron based results were in fair agreement with those obtained by other two control methods, while the second data set yielded comparable values of the principal direction only. Therefore, the proposed method, once automated, would offer the potential for scanning large volumes only if the following points are addressed successfully.

The evaluation of the orientation tensor components should be improved. Indeed, the proposed method tends to overestimate the values of the diagonal components of the fibre orientation tensor; this is mainly due to the uniform orientation of all the fibres in the subset which is implicitly assumed when using DIC and it is only partially mitigated by an averaging procedure over neighbouring subsets. This step of the procedure is the one that, in the authors' opinion, offers the best margins of improvement.

A filter for results to be excluded from the analysis when the correlation coefficient is too large proved to be efficient; however, the definition of the threshold to be set still needs further investigations in order to determine it without the need of a second method to check fibre orientations. Finally, the sample analysed herein was extracted from a relatively large flat plate, resulting into a uniform and almost planar FOD; for more complex FODs, a more complex algorithm, capable to scan all planes passing through a measuring point would be needed. This could also extend the applicability of the method to other SFRP materials, suitable for other manufacturing process than injection moulding.

Acknowledgements

Authors gratefully acknowledge Mr. L. Marta and Mr. L. Tentorio of SmartNDT, Villasanta MB, Italy, for micro-CT scans and fibre orientation measurements using VGStudio MAX

Bibliography

- [1] Fu S, Lauke B, Mai YW. Science and Engineering of Short Fibre Reinforced Polymer Composites. Elsevier Science; 2009.
- [2] Advani SG, Tucker III CL. The use of tensors to describe and predict fiber orientation in short fiber composites. *J Rheol* 1987; 31:751-84.
- [3] Fu S, Lauke B. Effects of fiber length and fiber orientation distributions on the tensile strength of short-fiber-reinforced polymers. *Compos Sci Technol* 1996; 56:1179-90.
- [4] Gupta M, Wang KK. Fiber orientation and mechanical properties of short-fiber-reinforced injection-molded composites: simulated and experimental results. *Polym Compos* 1993; 14:367-82.
- [5] Horst JJ. Influence of fibre orientation on fatigue of short glass fibre reinforced polyamide. Ph.D. thesis. TU Delft, Netherland; 1997.

- [6] Karger-Kocsis J, Friedrich K. Skin-core morphology and humidity effects on the fatigue crack propagation of PA-6.6. *Plast Rubber Compos Process Appl* 1989; 12:63-8.
- [7] Verweyst BE, Tucker III CL, Foss PH, Gara JFO. Fiber orientation in 3-D injection molded features: prediction and experiment. *International Polymer Processing* 1999; 14:409-420.
- [8] Bernasconi A, Davoli P, Basile A, Filippi A, Effect of fibre orientation on the fatigue behaviour of a short glass fibre reinforced polyamide-6, *Int J Fatigue* 2007; 29:199-208,
- [9] Müller T, Böhlke V. Prediction of effective elastic properties of fiber reinforced composites using fiber orientation tensors. *Compos Sci Technol* 2016; 130:36-45.
- [10] Darlington MW, McGinley PL, Smith GR. Structure and anisotropy of stiffness in glass fibre-reinforced thermoplastics. *J Mat Sci* 1976; 11:877-886.
- [11] Darlington MW, McGinley PL. Fibre orientation distribution in short fibre reinforced plastics. *J Mat Sci* 1975; 10:906-910.
- [12] Fakirov S, Fakirova C. Direct determination of the orientation of short glass fibers in an injection molded poly(ethylene terephthalate) system. *Polym Compos* 1985; 6:41-46.
- [13] Hine PJ, Davidson N, Duckett RA, Ward IM. Measuring the fibre orientation and modelling the elastic properties of injection-moulded long-glass-fibre-reinforced nylon. *Compos Sci Technol* 1995; 53:125-131.
- [14] Mlekusch B, Lehner EA, Geymayer W. Fibre orientation in short-fibre-reinforced thermoplastics I. Contrast enhancement for image analysis. *Compos Sci Technol* 1999; 59:543-545.
- [15] Bay RS, Tucker III CL. Stereological measurement and error estimates for three-dimensional fiber orientation. *Polym Eng Sci* 1992; 32:240-53.

- [16] Eberhardt C, Clarke A, Vincent M, Giroud T, Flouret S. Fibre-orientation measurements in short-glass-fibre composites II. A quantitative error estimate of the 2D image analysis technique. *Compos Sci Technol* 2001; 61:1961-1974.
- [17] Clarke A, Davidson N, Archenhold G. Measurements of fibre direction in reinforced polymer composites. *J Microsc* 1993; 171:69-79.
- [18] Jung SW, Kim SY, Nam HW, Han KS. Measurements of fiber orientation and elastic-modulus analysis in short-fiber-reinforced composites. *Compos Sci Technol* 2001; 61:107-116.
- [19] McGrath JJ, Wille JM. Determination of 3d fibre orientation distribution in thermoplastic injection molding. *Compos Sci Technol* 1995; 53:133-143.
- [20] Davidson NC, Clarke AR, Archenhold G. Large-area, high resolution image analysis of composite materials. *J Microsc* 1997; 185:233-242.
- [21] Clarke AR, Archenold G, Davidson NC. A novel technique for determining the 3D spatial distribution of glass fibres in polymer composites. *Compos Sci Technol* 1995; 55:75-91.
- [22] Eberhardt CN, Clarke AR. Fibre-orientation measurements in short-glass-fibre composites. Part I: automated, high-angular-resolution measurement by confocal microscopy. *Compos Sci Technol* 2001; 61:1389-1400.
- [23] Régnier G, Dray D, Jourdain E, Roux SL, Schmidt FM. A simplified method to determine the 3D orientation of an injection molded fiber-filled polymer. *Polym Eng Sci* 2008; 48:2159-2168.
- [24] Eberhardt CN, Clarke AR. Automated reconstruction of curvilinear fibres from 3D datasets acquired by X-ray microtomography. *J Microsc* 2002; 206:41-53.

- [25] Shen H, Nutt S, Hull D. Direct observation and measurement of fiber architecture in short fiber-polymer composite foam through micro-CT imaging. *Compos Sci Technol* 2004; 64:2113-2120.
- [26] Salaberger D, Kannappan KA, Kastner J, Reussner J, Auinger T. Evaluation of Computed Tomography Data from Fibre Reinforced Polymers to Determine Fibre Length Distribution. *Int Polym Process* 2011; 26:283-291.
- [27] Hessman PA, Riedel T, Welschinger F, Hornberger K, Böhlke T, Microstructural analysis of short glass fiber reinforced thermoplastics based on x-ray micro-computed tomography, *Composites Science and Technology*, Volume 183, 2019, 107752
- [28] Sun X, Lasecki J, Zeng D, Gan Y, Su X, Tao J. Measurement and quantitative analysis of fiber orientation distribution in long fiber reinforced part by injection molding. *Polym Test* 2015; 42:168-174.
- [29] Nguyen TB, Morioka M, Yokoyama A, Hamanaka S, Yamashita K, Nonomura C. Measurement of fiber orientation distribution in injection-molded short-glass-fiber composites using X-ray computed tomography. *J Mater Process Technol* 2015; 219:1-9.
- [30] Bernasconi A, Cosmi F, Dreossi D. Local anisotropy analysis of injection moulded fibre reinforced polymer composites. *Compos Sci Technol* 2008; 68:2574-2581.
- [31] Bernasconi A, Cosmi F, Hine PJ. Fibre orientation distribution in short fibre reinforced polymers: A comparison between optical and tomographic methods. *Compos Sci Technol* 2012; 72: 2002-2008.
- [32] Wirjadi O, Schladitz K, Rack A, Breuel T. Applications of anisotropic image filters for computing 2D and 3D-fiber orientations. *Image Anal Stereol* 2009; Proceedings of the ECS 09.

- [33] Altendorf H, Jeulin D. 3D directional mathematical morphology for analysis of fiber orientations. *Image Anal Stereol* 2009; 28:143-153.
- [34] Krause M, Hausherr JM, Burgeth B, Herrmann C, Krenkel W. Determination of fibre orientation in composites using the structure tensor and local X-ray transform. *J Mat Sci* 2010; 45: 888-896.
- [35] Straumit I, Lomov SV, Wevers M. Quantification of the internal structure and automatic generation of voxel models of textile composites from X-ray computed tomography data *Compos Part A Appl Sci Manuf*, 69 (2015), pp. 150-158
- [36] Karamov R, Martulli LM, Kerschbaum M, Sergeichev I, Swolfs Y, Lomov SV, Micro-CT based structure tensor analysis of fibre orientation in random fibre composites versus high-fidelity fibre identification methods, *Composite Structures*, 2020
- [37] Pinter P, Dietrich S, Bertram B, Kehrer L, Elsner P, Weidenmann KA. Comparison and error estimation of 3D fibre orientation analysis of computed tomography image data for fibre reinforced composites. *NDT&E Int* 2018; 95:26-35.
- [38] Wirjadi O, Schladitz K, Easwaran P, Ohser J. Estimating fibre direction distributions of reinforced composites from tomographic images. *Image Anal Stereol* 2016; 35:167-179.
- [39] Yoshimura A, Hosoya R, Koyanagi J, Ogasawara T. X-ray computed tomography used to measure fiber orientation in CFRP laminates. *Advan Compos Mater* 2016; 25:19-30.
- [40] Iizuka K, Ueda M, Takahashi T, Yoshimura A, Nakayama M. Development of a three-dimensional finite element model for a unidirectional carbon fiber reinforced plastic based on X-ray computed tomography images and the numerical simulation on compression, *Advanced Composite Materials* 2019, 28:1, 73-85

- [41] Takahashi T, Ueda M, Iizuka K, Yoshimura A, Yokozeki T. Simulation on kink-band formation during axial compression of a unidirectional carbon fiber-reinforced plastic constructed by X-ray computed tomography images, *Advanced Composite Materials* 2019, 28:4, 347-363
- [42] Pan B, Qian K, Xie H, Asundi A. Two-dimensional digital image correlation for in-plane displacement and strain measurement: a review. *Meas Sci Technol* 2009; 20:1-17.
- [43] Cosmi F, Bernasconi A, Sodini N, Phase contrast micro-tomography and morphological analysis of a short carbon fibre reinforced polyamide, *Composites Science and Technology*, 2011 (71); 23-30,
- [44] Kastner J, Plank B, Reh A, Salaberger D, Heinzl C, *Advanced X-Ray Tomographic Methods for Quantitative Characterisation of Carbon Fibre Reinforced Polymers*. 4th International Symposium on NDT in Aerospace 2012 Augsburg, Germany.
- [45] Bernasconi A. Cosmi F. Analysis of the dependence of the tensile behaviour of a short fibre reinforced polyamide upon fibre volume fraction, length and orientation. *Procedia Engineering* 2011; 10: 2129-2134